Miscibility and Physical Properties of Conducting Poly(urea-urethane) Thermoplastic Elastomers

Jia-Yi Liu, Chao-Chen Yang, Yen-Zen Wang

*Graduate School of Engineering Science and Technology (Doctoral Program),
National Yunlin University of Science and Technology, Yunlin 640, Taiwan*

ABSTRACT: A series of amine-terminated polyaniline oligomer (OPA)-based conducting poly(urea-urethane) thermoplastic elastomers (PUUs) was synthesized by two-stage solution polymerization and characterized by FTIR. Various percentages of OPA were introduced into PUUs as chain extenders to form hard segments of PUUs with urea-linkages. Spectroscopic and differential scanning calorimetry, as well as dynamic mechanical analysis, were conducted to elucidate the interaction and degree of miscibility between hard and soft segments, which were related to the stress–strain properties of PUUs. The hydrogen bonding index (HBI) measured by FTIR was employed to show the degree of interchain hydrogen bonding. Copolymer films with higher OPA content exhibit higher HBI and the degree of miscibility is significantly improved. The resultant conducting copolymers have higher tensile strength, higher Young's modulus, and lower elongation at break, because of the long rigid structure of OPA and the increase in the number of hydrogen bonds among the copolymers blocks. Incorporating OPA in PUUs increases the mass of the residue at temperatures over 600°C, according to thermogravimetric analysis. The conductivity of PUUs is found to range from 0.83 S/cm for neat OPA to 6.11×10^{-5} S/cm for PUUs. © 2006 Wiley Periodicals, Inc. J Appl Polym Sci 103: 3803–3810, 2007

Key words: miscibility; physical property; copolymer; poly(urea-urethane); polyaniline oligomer

INTRODUCTION

Elastomers formed by introducing conductive additives with high electrical conductivity have important applications in seals between pipes for transferring flammable gases, electromagnetic shielding, corrosion inhibition, and sensors.[1–4] Thermoplastic polyurethane (TPU) elastomers are versatile and can be easily prepared by a simple polyaddition reaction of polyol, diisocyanate, and a chain extender. The physical properties of TPU appear to be determined by a combination of the chain segment mobility, the rigidity of the aromatic units, chain entanglement, hydrogen bonding, and other intermolecular interactions.[5] The incompatibility between the hard segment and the soft segment causes polyurethanes (PUs) to undergo microphase separation to yield a hard-segment domain, a soft-segment matrix, and urethane-bonded interphase. The primary driving force of the phase separation depends on intermolecular hydrogen bonding between the hard segments of the urethane and the urea linkages.[6–9] Hydrogen bonding in PUs has been extensively studied using infrared spectroscopy.[10–14] The magnitude of the shift in the wavenumber indicates the hydrogen bonding strength. Traditionally, conductive additives, such as carbon black, metallic fibers, and conducting polymer are used. Polyaniline (PANI) is one of the most fascinating conductive polymers because of its environmental stability, ease of preparation, and the possibility of controlling its electrical conductivity via a unique doping process. However, the stiffness of the chain makes processing difficult, since the doped PANI is insoluble in common organic solvents and its mechanical properties are not suitable for many applications. This problem has been extensively addressed. Three main approaches have been developed: the incorporation of substituents into the chain, the formation of conductive blends/composites and the copolymerization method. The blending of PANI with other polymers is a highly active area of research, with numerous publications in recent years, aimed at combining favorable mechanical properties with high electrical conductivity.[15–22] One of the major limitations of the blending is that it always generates a highly heterogeneous phase-separated morphology. Therefore, blending composites to reach molecular intermixing is extremely difficult, such mixing is required to improve significantly the physical properties of the blend. The molecular intermixing of the two components can be manipulated via copolymerization or using a cured network. Examples of copolymers that contain aniline

include the grafting polyacrylic acid or polyethylene glycol onto a PANI backbone[23,24] and blocked structures such as PU-PANI octamer.[25] The interconnection of PANI chains through PU segments has yielded a series of new semiconducting materials with favorable mechanical properties.[26] Recent advances have led to the synthesis of aniline-oligomers (OPA) with controllable molecular weights and architectures.[27–31] Aniline-oligomers with well-defined end-groups may have high solubility and be able to undergo further polymerization.[32] The resultant polymers exhibit better processability and mechanical properties.[26] In this work, the chemical method that involves the copolymerization of the PU prepolymer and OPA is utilized to improve the processability, the degree of miscibility, the mechanical properties, the thermal stability, and the conductivity of the doped copolymers.

EXPERIMENTAL

Preparation of amine-terminated polyaniline oligomer powders

Aniline (9.5 g) and 24.3 g of ammonia persulfate (APS) were dissolved in 150-mL aqueous solution of $1M$ HCl and 350-mL aqueous solution of $1M$ HCl, respectively, and stored separately in a refrigerator overnight. An appropriate p-phenylene diamine (p-PDA) (about 1.12 g) was mixed with aniline solution before APS aqueous solution was added dropwise to the aniline solution and the mixture was maintained at 0–5°C for 24 h with continuous stirring, to control the molar mass.[33] The resulting OPA was isolated by filtration and dedoped by stirring in a $0.1M$ aqueous solution of ammonia for 12 h. The cake was dried in a dynamic vacuum oven for 3 days and ground into powder using a mortar. The molar mass and molar mass distribution of the resulting OPA were measured using a gel permeation chromatographer (GPC, Testhigh model 500) with monodistributed polystyrene as the standard. The number average molecular weight and molecular weight distribution expressed

as polydispersity index of the OPA were measured by gel permeation chromatograph and it turned out to be 1380 and 1.69, respectively.

Preparation of NCO-terminated PU-prepolymer solution

PU-prepolymer was prepared with a 2 : 1 mol ratio of purified MDI (4-4′-diphenylmethane diisocyanate) to polyol[poly(butylene adipate)glycol] (PBA) with molecular weights of 1000 and 2000, respectively, at 70°C under gaseous nitrogen with stirring until the desired extent of reaction was reached.[34] The change of the NCO content during reaction was determined using a standard dibutylamine back-titration method (ASTM D1638). These reactions of PBA1000-based PU-prepolymer and PBA2000-based PU-prepolymer were allowed to process for 2 and 3.5 h, respectively.

Preparation of amine-terminated polyaniline oligomer-based conducting poly(urea-urethane) thermoplastic elastomers

OPA was dissolved in N-methyl pyrrolidone (NMP). The resulting PU-prepolymer in NMP was mixed with an equivalent amount of OPA–NMP mixture plus a chain extender (1,4-butanediol) at 70°C until the —NCO groups disappeared, and then it was dried under dynamic vacuum at 50°C for 3 days (first dried procedure; FDP). The molar ratio of the OPA to the chain extender (as shown in the Table I) was varied to control the OPA block content in the copolymers while keeping the total amount equal to that of the PU-prepolymers. The resultant copolymers were further dried under dynamic vacuum at 90°C for 2 days (second dried procedure; SDP) to remove the residual solvent and water. Table I presents the compositions of resultant copolymers.

FTIR spectrum

FTIR spectra of dry films were obtained by a Perkin–Elmer FTIR (Fourier-transform infrared spectroscopy-

TABLE I
Designation and Composition of OPA-Based Conducting Poly(urea-urethane) Thermoplastic Elastomers

OPA-based poly (urea-urethane) copolymers	Polyol employed	Polyol molecular weight	OPA (wt %)	OPA/1,4BD (mole ratio)
PUB1OPA0	PBA	1000	0	0
PUB1OPA10	PBA	1000	10	0.15
PUB1OPA20	PBA	1000	20	0.40
PUB1OPA30	PBA	1000	30	1.04
PUB2OPA0	PBA	2000	0	0
PUB2OPA10	PBA	2000	10	0.26
PUB2OPA20	PBA	2000	20	0.88
PUB2OPA30	PBA	2000	30	2.28

mode: spectrum one) spectrometer. Thirty-two scans from 400 to 4000 cm^{-1} were performed on a pellet sample of KBr powder with a resolution of 2 cm^{-1}. The absorption peak due to hydrogen-bonded C=O stretching is centered at 1703 cm^{-1} and that due to free C=O stretching is centered at $\sim$ 1730 cm^{-1}. The extent of the carbonyl absorption group participating in hydrogen bonding is expressed by the hydrogen bonding index (HBI), which is the relative absorbances of the hydrogen-bonded carbonyl peak to that of free hydrogen-bonded carbonyl peak.[35–37]

Conductivity

The resistance (R) of the material was measured using a four-probe measurement instrument and the conductivity was obtained from the formula $\sigma = \frac{L}{(RA)}$, where L denotes the thickness and A is the cross section area.[38] Each sample was pressed into a pellet (diameter: $\sim$ 1.3 cm; thickness: $\sim$ 1.5 mm). At least five samples were employed to yield the final data by averaging.

Mechanical testing

Samples of size $50 \times 10 \times 0.25$ mm^3 were prepared and tested in a Tensilon machine (mode TCF-RC) made by Yashima Works (Tuichung, Taiwan). At least five samples were employed to yield the final data by averaging. The speed of testing machine crossheads was adjusted to 25 mm/min. The mechanical properties of the samples are represented in the table and are also represented graphically.

Differential scanning calorimetry

Differential scanning calorimetry (DSC) was performed using a DuPont Q100 MDSC instrument. The samples were heated from -120 to $200°C$ in an atmosphere of N_2 at a heating rate of $20°C/min$.

Dynamic mechanical analysis

Storage modus (E'), loss modus (E''), and tan δ of the samples were obtained from a DuPont 2980 DMA at $3°C/min$ from -120 to $200°C$. The sample was of dimension $50 \times 8 \times 0.25$ mm^3, and the damping mode and frequency were the extension mode and 1 Hz, respectively.

Thermogravimetric analysis

The thermogravimetric analysis (TGA) of the samples was carried out using a DuPont Q500 TGA instrument. The analysis was performed at a heating rate of $10°C/min$ in an atmosphere of nitrogen.

RESULTS AND DISCUSSION

Analyses by FTIR spectroscopy

The PU-prepolymer, OPA, and PUUs were characterized by FTIR, yielding the results presented in Figure 1. The strong peak at $\sim$ 3400–3500 cm^{-1}, presented in Figure 1 (curve a), from the OPA is associated with the imino group of OPA. The stretching modes of benzoid and quinoid reveal strong absorptions at 1590 and 1502 cm^{-1}, respectively. Figure 1 (curves b and c) shows typical FTIR spectra of PUUs and the PBA-based PU-prepolymer, respectively. Figure 1 (curve c) presents a strong and sharp peak at $\sim$ 3400–3500 cm^{-1} associated with the stretching vibration of the N—H bond, strong absorption peaks at $\sim$ 1700–1730 cm^{-1} associated with the stretching vibration of the C=O bond in the urethane, and an —NCO strong peak at 2270 cm^{-1}. However, the FTIR spectra of the PUUs [Fig. 1 (curve b)] include a moderately strong peak at about 1645 cm^{-1} due to the urea bond,[7,39] and the disappearance of two peaks at 2270 cm^{-1} and 3400–3500 cm^{-1} is caused by the formation of urea in the reactions of the —NCO group with the —NH$_2$ group of the OPA, which yields two absorption peaks at 1015 and 1495 cm^{-1} that are associated with the symmetric and asymmetric stretching vibrations of N—C—N in the resultant copolymers, respectively.[40] Rest absorption peaks are assigned in Table II.[40,41] Figure 2 displays scale-expanded FTIR spectra (1650 and 1750 cm^{-1}) of PUUs with various OPA contents. As shown in Figure 2, the major carbonyl stretching bands of PUUs under dynamic vacuum at $50°C$ are observable.[42] It is noted that the carbonyl peaks of PUUs mainly include two characteristic peaks :the one at about 1700 cm^{-1} resulting
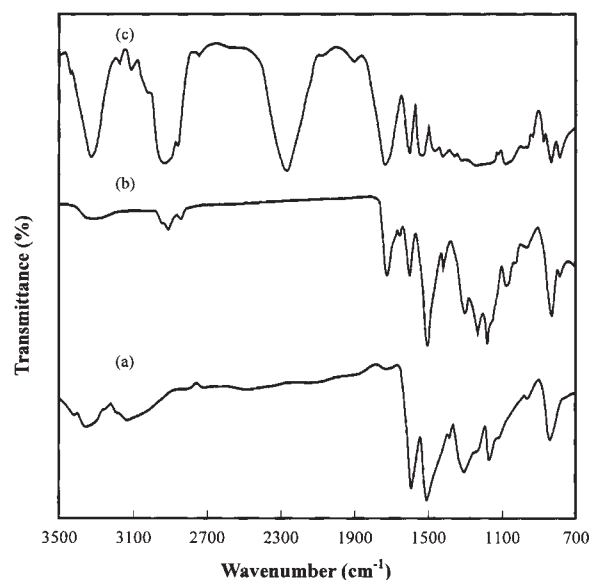

Figure 1 FTIR spectra of (a) OPA; (b) PUB1OPA20; (c) PUB1OPA0 prepolymer.

TABLE II
Characteristic FTIR Absorptions of OPA-Based Conducting Poly(urea-urethane) Thermoplastic Elastomers

Functional group	Wavenumber (cm^{-1})	Comments
Imines	3444	Free N—H stretching
—CH$_3$	2958	Symmetric
—CH$_2$—	2924	Asymmetric
—C=O	1739–1729	Free urethane carbonyl
—C=O	1713–1706	H-bonded urethane carbonyl
—C=O	1700	Free urea carbonyl
—C=O	< 1700	H-bonded urea carbonyl
—C=C—	1600	Benzene ring, usually $\sim$ 1600 cm^{-1}
N—H+C—N	1540	Amide band
—C=N—	1590	Quinoid
—C=C—	1497	Benzoid
H—C—N	1490–1465	Asymmetric
(—C—N—)	1300	Stretching in QBQ
—N—Q—N—	1164	Stretching
—B—NH—B—	1124	
—C—O—C—	1110	Asymmetric ether group
N—C—N	$\sim$ 1010	Symmetric
C—H	801	*para*-Substituted aromatic out-of-plain bending

from self-association of N—H with C=O in the interior of hard domains, and the other, at about 1730 cm^{-1}, is related to the free carbonyl group. As OPA content increases, the stretching band of the free carbonyl group broadens gradually and shifts to a lower wavenumber that is caused by intermolecular and intermolecular H-bonding in these copolymers. Additionally, a carbonyl stretching band at about 1710 cm^{-1} that is assigned to carbonyl group stretching with water molecules[43] is observed. To make out the interaction form of the residual water molecules in PUUs, the samples were further dried under dynamic vacuum at higher
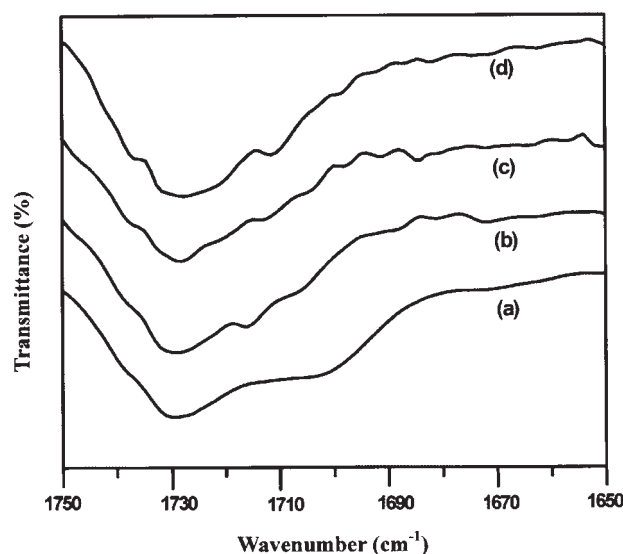
temperature ($\sim$ 90°C) and analyzed with FTIR spectroscopy. Figure 3 presents FTIR spectra of PUUs under dynamic vacuum at various temperatures. Compared to Figure 3 (curves a and b), the carbonyl stretching band at 1710 cm^{-1} is almost disappeared [as shown in Fig. 3 (curve b)]. The phenomenon suggests that the residual water molecules in PUUs can be effectively removed by vacuum-drying at a higher temperature. To avoid interference of various contents of water molecules in PUUs, a SDP was used to prepare tested samples of FTIR analyses. As mentioned above, the extent of the carbonyl group participating in hydrogen bonding is expressed by HBI, which is defined as the relative absorbances of two carbonyl peaks.[35]

$$HBI = A_{C=O,bonded}/A_{C=O,free} \qquad (1)$$

where $A_{C=O,bonded}$ and $A_{C=O,free}$ are the absorbances of bonded and free carbonyl group, respectively. All these carbonyl group wavenumbers of PUUs, prepared under dynamic vacuum at the higher temperature, split into two bands at 1730 and 1700 cm^{-1}, corresponding to the free and the hydrogen-bonded carbonyl group, which can be fitted well to the Gaussian function.[44,45] The HBI can be calculated from eq. (1) resulting from curve-fitting of absorbances of two carbonyl peaks. Table III summarizes the HBI of PUUs. The HBI of PUUs is found to range from 0.9 for neat PU to 1.37 for PUUs. This result indicates that the HBI increases with the increase of the OPA content in the PUUs. The greater HBI values indicate increased participation of the carbonyl group in hydrogen bonding and the lower the degree of segregation between hard and soft segments.

Thermal property

Thermal analyses by DSC and DMA are performed to determine the glass transition temperature (T_g) and

Figure 2 FTIR spectra of (a) PUB1OPA0; (b) PUB1OPA10; (c) PUB1OPA20; (d) PUB1OPA30.
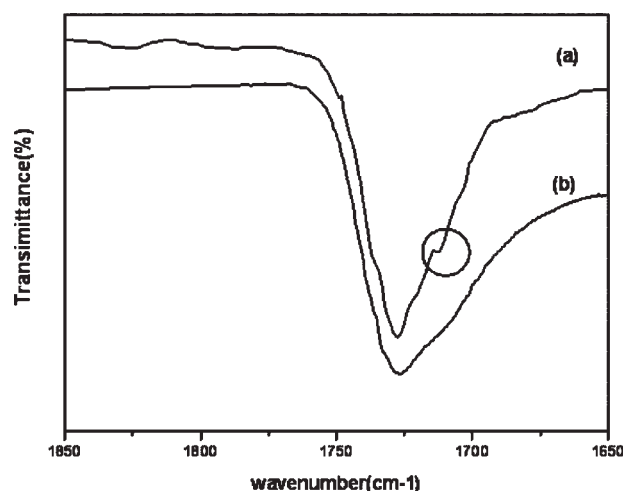

Figure 3 FTIR spectra of PUB1OPA20; (a) FDP, (b) SDP.

TABLE III
HBI and Glass-Transition Temperature of OPA-Based Conducting
Poly(urea-urethane) Thermoplastic Elastomers Obtained from DMA

Aniline-containing poly(urea-urethane) conducting copolymers	$HBI = A_{C=O,bonded}/A_{C=O,free}$	T_g (°C)	
		From tan δ peak vs. temperature plot	From E'' peak vs. temperature plot
PUB1OPA0	0.90	−13	−20
PUB1OPA10	1.10	−6	−18
PUB1OPA20	1.14	−5	−15
PUB1OPA30	1.32	6	−13
PUB2OPA0	0.99	−34	−37
PUB1OPA10	1.10	−33	−36
PUB2OPA20	1.19	−29	−28
PUB2OPA30	1.37	−28	−27

miscibility of PUUs. The T_g of the PUUs with various OPA contents was measured by DSC and DMA, as displayed in Figures 4 and 5, respectively. The lines in Figure 4(a,b) that are labeled (a) represent the DSC thermograms of neat PBA-based PU with polyol with various molecular weights. The T_g values of the PBA-based PUs are about −33°C (PBA1000) and −48°C (PBA2000), respectively. The T_g of OPA could not be determined from the DSC thermograms, since the OPA decomposes below its T_g or melting temperature. As shown in Figure 4 for the PUUs with various OPA contents, the T_g of the soft domain in the block copolymers increases with their OPA content. The increase in T_g of the copolymers is measured to be about 15°C when the OPA content of the block copolymer exceeds 30%, revealing that the miscibility between the urethane and the OPA of the copolymers of the covalently bonded blocks is significantly better than that of the noncovalently bonded blends.

Figures 5(a, b) shows the dynamic storage modulus (E') as a function of temperature for PUUs at different OPA compositions. The energy requirement for storage measurement was related to the stiffness of the specimens. All samples showed a glass-state plateau region. As expected, the modulus of samples below glass transition temperature was slightly increased with increasing temperature. However, the modulus increased markedly as OPA content increased from 10 to 30 wt %. This behavior will be associated with the hydrogen bond strength in PUUs. It is well known that the NH groups in urethane and the urea linkages form a hydrogen bond with the carbonyl group of hard segment or with an ester group of soft segment. The curves of the temperature dependence of the tan δ of the PUUs with various OPA contents were determined by DMA and presented in Figures 5(c) and 5(d). The tan δ curves of neat PU and PUUs exhibit one relaxation peak. The relaxation peak is assigned to the T_g of the soft-segment-rich regions of neat PU or PUUs. The T_g values associated with the tan δ peak are summarized in Table III. The data show that T_g are dependent on the OPA composition in the PUUs.
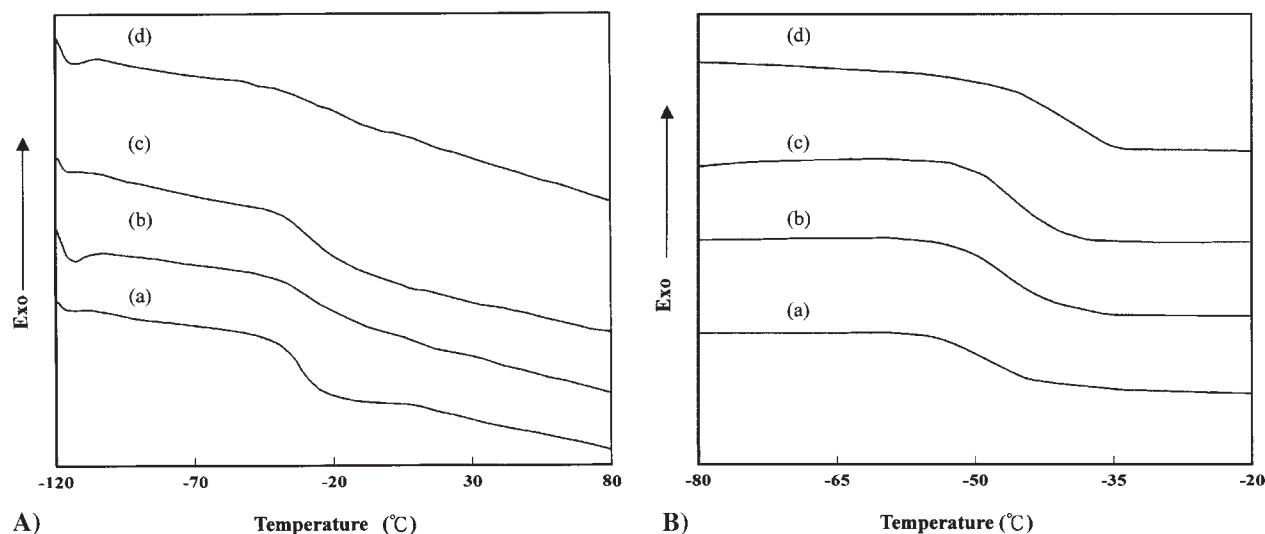

Figure 4 DSC thermograms of OPA-based conducting poly(urea-urethane) thermoplastic elastomers. (A): (a) PUB1OPA0; (b) PUB1OPA10; (c) PUB1OPA20; (d) PUB1OPA30. (B): (a) PUB2OPA0; (b) PUB2OPA10; (c) PUB2OPA20; (d) PUB2OPA30.
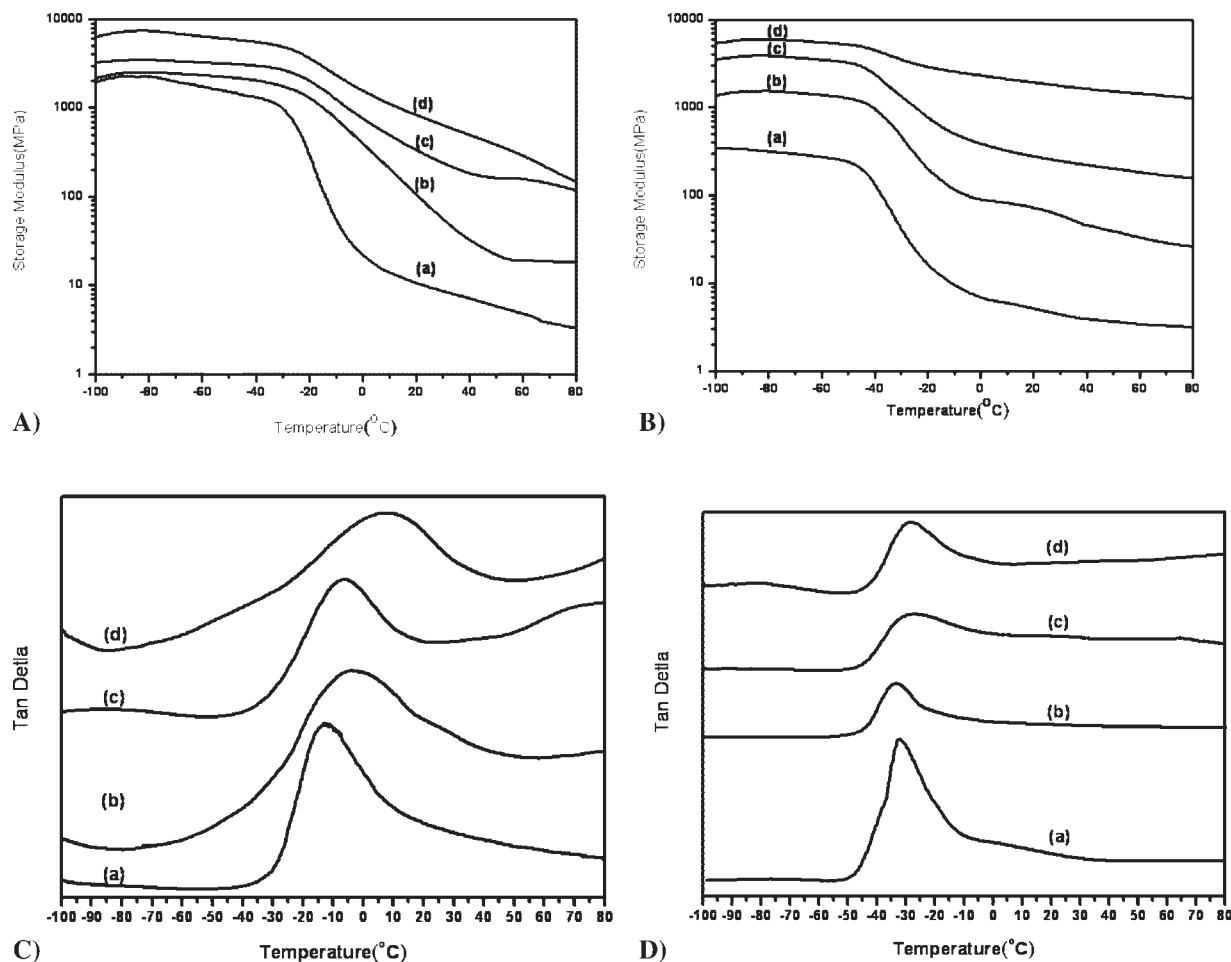
Figure 5 DMA thermograms (E') of OPA-based conducting poly(urea-urethane) thermoplastic elastomers: (A): (a) PUB1OPA0, (b) PUB1OPA10, (c) PUB1OPA20, (d) PUB1OPA30; (B): (a) PUB2OPA0, (b) PUB2OPA10, (c) PUB2OPA20, (d) PUB2OPA30; DMA thermograms (tan δ) of OPA-based conducting poly(urea-urethane) thermoplastic elastomers: (C): (a) PUB1OPA0, (b) PUB1OPA10, (c) PUB1OPA20, (d) PUB1OPA30; (D): (a) PUB2OPA0, (b) PUB2OPA10, (c) PUB2OPA20, (d) PUB2OPA30.

As OPA content of PUUs is increased, the T_g values increase. This trend is consistent with the E'' measurement. The T_g values of the copolymers increase with their OPA content, revealing that the miscibility between urethane and the OPA blocks increases with H-bonding, because of the covalent bonds in these two polymers, as revealed by the DSC thermograms and FTIR spectra.

The heat-resistivity is represented by the weight loss of PUUs with various OPA contents and was measured by TGA. Figure 6 presents the results. The degradation temperature, T_d, and the residual weight of the PUUs increase with the OPA content in the block copolymers. The residual weight of copolymers heated at over 600°C markedly exceeds that of neat PU, indicating that the PU molecules are prone to decompose in the block copolymer, and that the final residue char comes from the OPA in the resultant block copolymers.
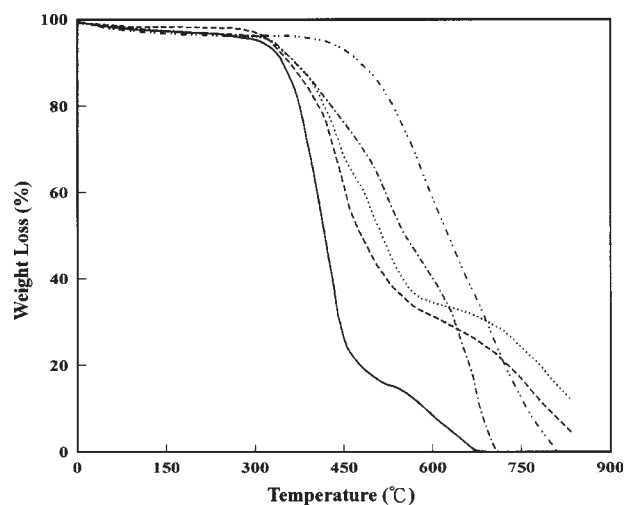

Figure 6 TGA thermograms of OPA-based conducting poly(urea-urethane) thermoplastic elastomers. ——: PUB1O-PA0; -------: PUB1OPA10; ……: PUB1OPA20; ------: PUB1OPA30; ----------: OPA.
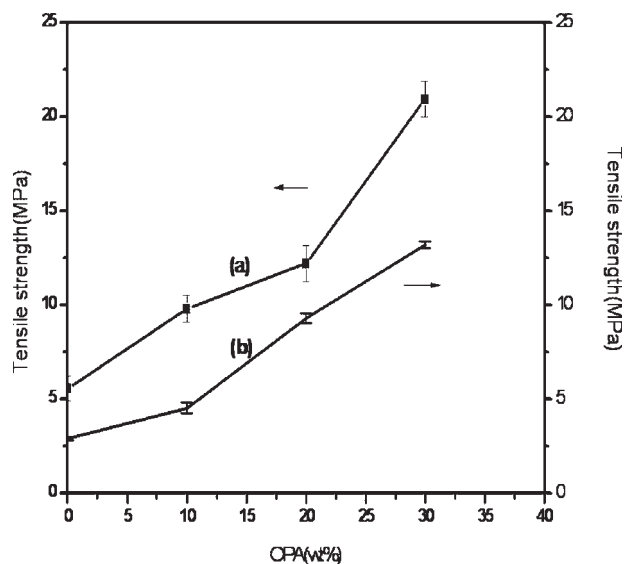
Figure 7 Dependence of the tensile strength of OPA-based copolymers on the OPA content; (a) PBA1000-based PUUs, (b) PBA2000-based PUUs.

Conductivity and mechanical property

Figure 7 shows the dependence of the tensile strength of the OPA-based copolymers on OPA content. Table IV presents the measured values of the conductivity, tensile strength, Young's modulus, and elongation at break of PUUs. From Figure 7 and Table IV, it is observed that the sample (PUB1OPA0 or PUB2OPA0) containing only 1,4-butanediol displays a lower Young's modulus and tensile strength and behaves like a typical elastomer with a large elongation at break. The incorporation of OPA segments along the chain backbone leads to a distinctly higher tensile strength and Young's modulus and lower elongation at break. Since several benzene rings are attached to the OPA backbone, the tensile strength and Young's modulus of the PUUs surprisingly exceeds that of neat PU. In particular, the covalent bonds and intermolecular H-bonds between the OPA and the ure-

thane blocks are thought to dominate main contributors to the tensile strength and Young's modulus of the resultant copolymers, because they improve the miscibility between the blocks. The structure of the copolymer is very similar to that of the PU as both have alternating hard and soft segments on the backbones. In the regularly structured PU, the MDI (4,4'-diphenylmethane diisocyanate) linked with the chain extender (1,4-butanediol) forms the hard segment. However, in the PUUs, the hard segment comprises additional long and rigid OPA blocks that behave as molecular fibers. Hence, the hard segment acts not only as physical crosslinks but also as reinforced rigid-rod fibers in the soft-segment matrix to increase significantly the tensile strength of the block copolymer to a value similar to that of a molecular composite. The presence of more long and stiff OPAs in copolymers corresponds to higher tensile strength.

The conductivity of the block copolymers is found to range from 0.83 S/cm for OPA to 6.11×10^{-5} S/cm for the copolymers after doping with HCl. OPA, which behaves as a chain-extender, does not provide a well-defined continuous pathway for transporting charges. Therefore, some of the OPAs that are covalently bonded with PU blocks did not contribute to the increase in conductivity. The conductive OPA blocks in the copolymer are also diluted and separated by the nonconductive PU blocks along the backbones, constraining electric transfer between the PUU molecules. Based on the above-mentioned factors, the conductivity of PUUs is reduced by four orders of magnitude. The conductivity of the block copolymers increases with the OPA contents, in a manner similar to miscible polymer blends, because the OPA is randomly distributed and in contact with other OPA since the interaction between the blocks is improved, facilitating the transportation or jumping of electrons from one OPA block to another. The conductive OPA (the hard segments) block can subsequently come into contact with other OPA, forming a continuous conductive bridge even though the electron transfer is

TABLE IV
Conductivity and Mechanical Properties of OPA-Based Conducting Poly(urea-urethane) Thermoplastic Elastomers

Aniline-containing poly(urea-urethane) conducting copolymers	Conductivity (S/cm)	Tensile strength (MPa)	Elongation at break (%)	Young's modulus (MPa)
PUB1OPA0	–	5.56 ± 0.66	529 ± 20	19.2 ± 0.2
PUB1OPA10	$(6.17 \pm 0.25) \times 10^{-5}$	9.80 ± 0.72	131 ± 7	41.3 ± 1.0
PUB1OPA20	$(1.78 \pm 0.08) \times 10^{-4}$	12.20 ± 0.96	57 ± 4	188.6 ± 2.9
PUB1OPA30	$(3.12 \pm 0.17) \times 10^{-4}$	20.92 ± 0.94	15 ± 1	496.1 ± 12.1
PUB2OPA0	–	2.88 ± 0.08	970 ± 40	1.3 ± 0.1
PUB1OPA10	$(6.11 \pm 0.05) \times 10^{-5}$	4.53 ± 0.30	313 ± 15	2.2 ± 0.1
PUB2OPA20	$(1.87 \pm 0.11) \times 10^{-4}$	9.29 ± 0.27	138 ± 10	44.1 ± 0.9
PUB2OPA30	$(3.07 \pm 0.04) \times 10^{-4}$	13.20 ± 0.19	116 ± 7	53.4 ± 0.4
OPA	$(8.30 \pm 0.03) \times 10^{-1}$	–	–	–

restricted by the nonconductive covalent-bonding PU block along the main chains.

CONCLUSIONS

The introduction of OPA as a chain extender into the PU backbone can strongly affect the properties of the resultant amine-terminated polyaniline oligomer-based conducting poly(urea-urethane) thermoplastic elastomers by copolymerization between the urethane blocks and the OPA urea blocks. The miscibility between the blocks is significantly improved and the T_g increases with OPA content. The degree of phase separation and elongation at break are increased as HBI value decreased. The tensile strength and Young's modulus of the block copolymers increases significantly with OPA content in the copolymers because the self-reinforced and rigid OPA forms a molecular-composite structure, which improves the miscibility between the urethane and the OPA blocks.

References

1. Heeger, A. J. Synth Met 2002, 125, 23.
2. Akcelrud, L. Prog Polym Sci 2003, 28, 875.
3. Kraljic, M.; Mandic, Z.; Duic, L. J Corros Sci 2003, 45, 181.
4. Debarnot, D. N.; Epaillard, F. P. Anal Chim Acta 2003, 475, 1.
5. Szycher, M. Szycher's Handbook of Polyurethanes; CRC Press: Boca Raton, FL, 1999.
6. Koberstein, J. T.; Russell, T. P. Macromolecules 1986, 19, 714.
7. Wang, C. B.; Cooper, S. L. Macromolecules 1983, 16, 775.
8. Sung, C. S. P.; Schneider, N. S. Macromolecules 1975, 8, 68.
9. Sung, C. S. P.; Schneider, N. S. Macromolecules 1977, 10, 106.
10. Sung, C. S. P.; Schneider, N. S. Macromolecules 1980, 13, 177.
11. Wang, F. C.; Feve, M.; Lam, T. M.; Pascault, J. P. J Polym Sci Part B: Polym Lett 1968, 6, 2137.
12. Tanaka, T.; Yokoyama, T.; Yamaguchi, Y. J Polym Sci Part A: Polym Phys 1994, 32, 1305.
13. Zharkov, V. V.; Strikovsky, A. G.; Verteleskaya, T. E. Polymer 1993, 34, 938.
14. Teo, L. S.; Chen, C. Y.; Kuo, J. F. Macromolecules 1997, 30, 1793.
15. Jousseaume, V.; Morsli, M.; Bonnet, A.; Tesson, O.; Lefrant, S. J Appl Polym Sci 1998, 67, 1205.
16. Segal, E.; Haba, Y.; Narkis, M.; Siegmann, A. J Polym Sci Part B: Polym Phys 2001, 39, 611.
17. Abraham, D.; Bharathi, A.; Subramanyam, S. V. Polymer 1996, 37, 5295.
18. Yang, J.; Zhao, C.; Cui, D.; Hou, J.; Wan, M.; Xu, M. J Appl Polym Sci 1995, 56, 831.
19. Lee, W. J.; Kim, Y. J.; Kaang, S. Synth Met 2000, 113, 237.
20. Frisch, H. L.; Ma, J.; Song, H.; Frisch, K. C.; Mengnjoh, P. C.; Molla, A. H. J Appl Polym Sci 2001, 80, 893.
21. Jeon, B. H.; Kim, S.; Choi, M. H.; Chung, I. J. Synth Met 1999, 104, 1160.
22. Wang, Y. Z.; Hsu, Y. C.; Chou, L. C.; Hsieh, K. H. J Polym Res 2004, 11, 127.
23. Chen, Y.; Kang, K. L. Polymer 2000, 41, 3279.
24. Wang, P.; Tan, K. L.; Zhang, F.; Kang, E. T.; Neoh, K. G. Chem Mater 2001, 13, 581.
25. Wang, Y. Z.; Hsu, Y. C.; Wu, R. R.; Ka, H. M. Synth Met 2003, 132, 151.
26. Paula, C. R.; Leni, A. Polymer 2003, 44, 891.
27. Shacklette, L. W.; Wolf, J. F.; Gould, S.; Baughman, R. H. J Chem Phys 1988, 88, 3955.
28. Wei, Y.; Yang, C.; Wei, G.; Feng, G. Synth Met 1997, 84, 289.
29. Cao, Y.; Li, S. Z.; Xue, Z. J.; Guo, D. Synth Met 1986, 16, 305.
30. Conwell, E. M.; Duke, C. B.; Paton, A.; Jeyadev, S. J Chem Phys 1998, 88, 3331.
31. Lu, F. L.; Wudl, F.; Nowak, M.; Heeger, A. J. J Am Chem Soc 1986, 108, 8311.
32. Wei, Y.; Yang, C.; Ding, T. Tetrahedron Lett 1996, 37, 731.
33. Zhang, W. J.; Feng, J.; MacDiamid, H. G.; Epstein, A. J. Synth Met 1997, 84, 119.
34. Li, C.; Yu, X.; Speckhard, T. A.; Cooper, S. L. J Polym Sci Part B: Polym Phys 1988, 26, 2315.
35. Seymour, R. W.; Estes, G. M.; Cooper, S. L. Macromolecules 1970, 3, 579.
36. Coleman, M. M.; Skrovanek, D. J.; Hu, J.; Painter, P. C. Macromolecules 1988, 21, 59.
37. Huang, S. L.; Lai, J. Y. Eur Polym J 1997, 33, 1563.
38. Mattoso, L. H. C.; MacDiarmid, A. G.; Epstein, A. J. Synth Met 1994, 68, 1.
39. Ishihara, H.; Kimura, I.; Saito, K.; Ono, H. J Macromol Sci Phys 1974, 10, 591.
40. Socrates, G. Infrared Characteristic Group Frequencies; Wiley Interscience: Chichester, UK, 1980.
41. Tang, T.; Jing, X.; Wang, B.; Wang, F. Synth Met 1988, 24, 211.
42. Andreatta, A.; Smith, P. Synth Met 1993, 55, 1017.
43. Xu, Y.; Yan, C.; Ding, J.; Gao, C. Prog Org Coat 2002, 45, 331.
44. Kuo, S. W.; Wu, C. H.; Chang, F. C. Macromolecules 2004, 37, 192.
45. Kuo, S. W.; Chang, F. C. Macromolecules 2001, 34, 5224.